E2-2008-125

I. Zborovský[1], M. V. Tokarev[2]

NEW PROPERTIES OF z-SCALING: FLAVOR INDEPENDENCE AND SATURATION AT LOW z

Presented at the XXXVIII International Symposium on Multiparticle Dynamics, September 14–21, 2008, DESY, Hamburg, Germany

[1]Nuclear Physics Institute, Academy of Sciences of the Czech Republic, Řež, Czech Republic; E-mail: zborovsky@ujf.cas.cz
[2]Joint Institute for Nuclear Research, Dubna, Russia;
E-mail: tokarev@sunhe.jinr.ru

Зборовский И., Токарев М. В. E2-2008-125
Новые свойства z-скейлинга:
флэйворная независимость и насыщение при малых z

Проанализированы экспериментальные данные, полученные на ISR, RHIC и Tevatron, по инклюзивным сечениям частиц, рожденных в протон-(анти)протонных взаимодействиях при высоких энергиях в рамках концепции z-скейлинга. Установлены новые свойства скейлинговой функции $\psi(z)$ — флэйворная независимость и насыщение при малых z. Первая закономерность проявляется в постоянстве формы скейлинговой функции для различных типов рожденных адронов. Вторая указывает на выполаживание $\psi(z)$ при уменьшении z и нулевом наклоне в области $z < 0{,}1$. Обсуждается физический смысл модельных параметров и их связь с некоторыми термодинамическими величинами (энтропией, удельной теплоемкостью, температурой). Показано, что поведение спектров в области малых z контролируется параметром c, интерпретируемым как удельная теплоемкость среды, образующейся вместе с инклюзивной частицей. Отмечается, что режим насыщения функции $\psi(z)$, наблюдаемый при малых z, наиболее предпочтителен для поиска фазовых переходов адронной материи и изучения непертурбативных свойств КХД в протон-(анти)протонных столкновениях при высоких энергиях на U70, RHIC, Tevatron и LHC.

Работа выполнена в Лаборатории физики высоких энергий им. В. И. Векслера и А. М. Балдина ОИЯИ.

Препринт Объединенного института ядерных исследований. Дубна, 2008

Zborovský I., Tokarev M. V. E2-2008-125
New Properties of z-Scaling:
Flavor Independence and Saturation at Low z

Experimental ISR, RHIC, and Tevatron data on inclusive cross sections of particles produced in high energy proton–(anti)proton collisions are analyzed in the framework of z-scaling. New features of the scaling function $\psi(z)$ are established. These are flavor independence of $\psi(z)$ including particles with heavy flavor content and saturation at low z. Flavor independence means that the shape of the scaling function $\psi(z)$ is the same for different hadron species. Saturation corresponds to flattening of $\psi(z)$ for low $z < 0.1$. Relations of model parameters used in data z-presentation with some thermodynamical quantities (entropy, specific heat, temperature) are discussed. It is shown that behavior of particle spectra at low z is controlled by a parameter c interpreted as specific heat of the created medium associated with production of the inclusive particle. The saturation regime of $\psi(z)$ observed at low z is assumed to be preferable in searching for phase transitions of hadron matter and for study of nonperturbative QCD in high energy proton–(anti)proton collisions at U70, RHIC, Tevatron, and LHC.

The investigation has been performed at the Veksler and Baldin Laboratory of High Energy Physics, JINR.

Preprint of the Joint Institute for Nuclear Research. Dubna, 2008

1. INTRODUCTION

The production of particles with high transverse momenta from the collision of hadrons and nuclei at sufficiently high energies has relevance to constituent interactions at small scales. In this regime, it is interesting to search for new physical phenomena in elementary processes such as quark compositeness [1], extra dimensions [2], black holes [3], fractal space-time [4], etc. Other aspects of high energy interactions are connected with small momenta of secondary particles and high multiplicities. In this regime collective phenomena of particle production take place. The search for new physics in both regions is one of the main goals of investigations at Relativistic Heavy Ion Collider (RHIC) at BNL and Large Hadron Collider (LHC) at CERN [5]. Experimental data on particle production at high energy and multiplicity provide constraints for different theoretical models. Processes with high transverse momenta of produced particles are suitable for a precise test of perturbative Quantum Chromodynamics (QCD). The soft regime is preferred for verification of nonperturbative QCD and investigation of phase transitions in non-Abelian theories.

One of the methods allowing systematic analysis of data on inclusive cross sections over a wide range of the collision energies, multiplicity densities, transverse momenta, and angles of the produced particles is based on the z-scaling observed in high energy proton–(anti)proton collisions (see Ref. [6] and references therein). The approach to the description of the inclusive spectra reflects the principles of locality, self-similarity, and fractality of hadron interactions at a constituent level. It takes into account the structure of the colliding objects, interaction of their constituents, and processes of particle formation over a wide scale range. The analyzed data include processes which take place at nucleon scales as well as at small scales down to 10^{-4} fm. The presentation of experimental data in this approach is given in terms of the scaling function $\psi(z)$ and the scaling variable z. Both are constructed using the kinematical variables, the experimentally measured inclusive cross section $Ed^3\sigma/dp^3$, the multiplicity density $dN/d\eta$, and some model parameters which allow physical interpretation.

It was shown [6] that the scaling behavior of $\psi(z)$ is valid for different types of the produced hadrons. The scaling function demonstrates two regimes. The first one is observed in the high- and the second one in the low-p_T region. The

hard part of the inclusive spectra is described by the power law, $\psi(z) \sim z^{-\beta}$, with a constant value of β at large z. The self-similar features of particle production dictated by the z-scaling at large z give strong restriction on the asymptotic behavior of the spectra in the high-p_T region. This provides suitable constraints on phenomenology of parton distribution functions and fragmentation functions which are needed to verify the perturbative QCD in hadron collisions. The soft regime of particle production demonstrates flattening of the scaling function $\psi(z)$ for small z. The behavior of $\psi(z)$ at small z is of interest to study the nonperturbative QCD in the processes with low-p_T. We consider that this region is most preferable in searching for phase transitions and study of collective phenomena in multiple particle systems.

In this paper we show that in the high energy pp and $p\bar{p}$ collisions the shape of the scaling function at low z is independent of the type of the inclusive hadron including production of the hadrons with heavy flavor content. A saturation of $\psi(z)$ with decreasing z is observed. The single parameter c which controls the behavior of $\psi(z)$ at low z is interpreted as a specific heat of the produced medium. The scaling in pp and $p\bar{p}$ collisions is consistent with a constant value of c. Search for a possible change in this parameter is of interest especially for soft processes with high multiplicities. Such a change could be an indication of a phase transition in the matter produced in high energy collisions of both hadrons and nuclei.

The paper is organized as follows. A concept of the z-scaling and the method of construction of the scaling function $\psi(z)$ are briefly described in Sec. 2. The properties of energy, angular, and multiplicity independence of the scaling function are mentioned in Sec. 3. The flavor independence and saturation of $\psi(z)$ at low z are demonstrated in Sec. 4. A microscopic picture of the constituent subprocess is analyzed in Sec. 5. A relation of the scaling variable z to some thermodynamical quantities is discussed in Sec. 6. Here we consider possible manifestations of phase transitions and their effects to the parameters used in the z-presentation of inclusive spectra. Conclusions are summarized in Sec. 7.

2. z-SCALING

In this paper we follow the version of the z-scaling presented in Ref. [6]. Let us briefly remind the basic ideas of this concept. At sufficiently high energies, the collision of extended objects like hadrons and nuclei is considered as an ensemble of individual interactions of their constituents. The constituents are partons in the parton model or quarks and gluons in the theory of QCD. A single interaction of constituents is illustrated in Fig. 1.

Structures of the colliding objects are characterized by parameters δ_1 and δ_2. The constituents of the incoming hadrons (or nuclei) with masses M_1, M_2 and

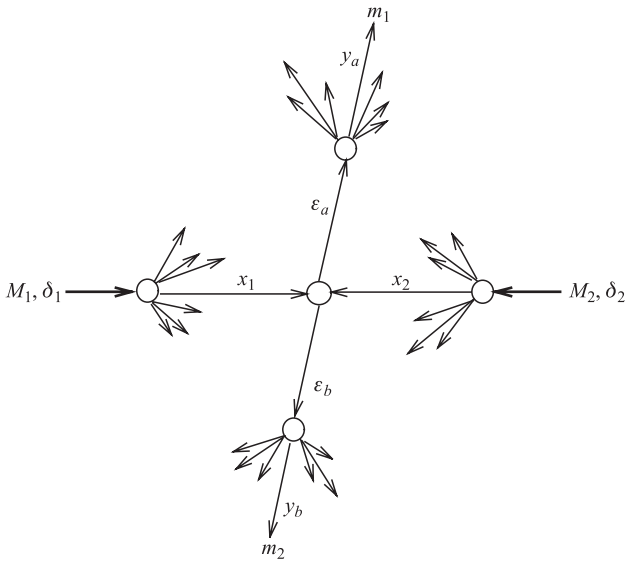

Fig. 1. Diagram of the constituent subprocess

momenta P_1, P_2 carry their fractions x_1, x_2. The inclusive particle carries the momentum fraction y_a of the scattered constituent with a fragmentation characterized by a parameter ϵ_a. A fragmentation of the recoil constituent is described by ϵ_b and the momentum fraction y_b. Multiple interactions are considered to be similar. This property represents a self-similarity of the hadronic interactions at the constituent level.

2.1. Momentum Fractions x_1, x_2, y_a, and y_b. The idea of the z-scaling is based on the assumption [7] that gross features of an inclusive particle distribution of the reaction

$$M_1 + M_2 \to m_1 + X \tag{1}$$

can be described at high energies in terms of the kinematical characteristics of the corresponding constituent subprocess. We consider the subprocess to be a binary collision

$$(x_1 M_1) + (x_2 M_2) \to (m_1/y_a) + (x_1 M_1 + x_2 M_2 + m_2/y_b) \tag{2}$$

of the constituents $(x_1 M_1)$ and $(x_2 M_2)$ resulting in the scattered (m_1/y_a) and recoil $(x_1 M_1 + x_2 M_2 + m_2/y_b)$ objects in the final state. The produced secondary objects transform into real particles after the constituent collisions. The registered particle with the mass m_1 and the 4-momentum p and its hadron counterpart, moving in the opposite direction, carry the momentum fractions y_a and y_b of the

scattered and recoil systems, respectively. The momentum conservation law of the constituent subprocess is connected with a recoil mass which we write in the form

$$(x_1P_1 + x_2P_2 - p/y_a)^2 = (x_1M_1 + x_2M_2 + m_2/y_b)^2. \quad (3)$$

The associate production of (m_2) ensures conservation of the additive quantum numbers. Equation (3) is an expression of the locality of the hadron interaction at a constituent level. It represents a kinematical constraint on the momentum fractions x_1, x_2, y_a, and y_b which determine a subprocess (2).

Structure of the colliding objects and fragmentation of the systems formed in the scattered and recoil directions are characterized by the parameters δ_1, δ_2 and ϵ_a, ϵ_b, respectively. We connect the structural parameters with the corresponding momentum fractions by the function

$$\Omega(x_1, x_2, y_a, y_b) = (1 - x_1)^{\delta_1}(1 - x_2)^{\delta_2}(1 - y_a)^{\epsilon_a}(1 - y_b)^{\epsilon_b}. \quad (4)$$

Physical interpretation of Ω is given by its proportionality to relative number of all such constituent configurations in reaction (1) which contain the configuration defined by the fractions x_1, x_2, y_a, and y_b. The function Ω plays the role of a relative volume which occupy these configurations in the space of the momentum fractions. It was found that the structural parameters δ_1, δ_2, ϵ_a, and ϵ_b have constant values at high energies. They are interpreted as fractal dimensions in the corresponding space of the momentum fractions. For proton–proton collisions we set $\delta_1 = \delta_2 \equiv \delta$. In the case of nucleus–nucleus collisions there are relations $\delta_1 = A_1\delta$ and $\delta_2 = A_2\delta$, where A_1, A_2 are atomic numbers [8]. We assume that the fragmentation of the objects moving in the scattered and recoil directions can be described by the same parameter $\epsilon_a = \epsilon_b \equiv \epsilon_F$ which depends on the type (F) of the inclusive particle. For given values of δ and ϵ_F, we determine the fractions x_1, x_2, y_a, and y_b in a way to maximize the function $\Omega(x_1, x_2, y_a, y_b)$, simultaneously fulfilling condition (3). The momentum fractions x_1 and x_2 obtained in this way can be decomposed as follows:

$$x_1 = \lambda_1 + \chi_1, \quad x_2 = \lambda_2 + \chi_2, \quad (5)$$

where $\lambda_{1,2} = \lambda_{1,2}(y_a, y_b)$ and $\chi_{1,2} = \chi_{1,2}(y_a, y_b)$ are simple specific functions [6] of y_a and y_b. Using the decomposition, the subprocess (2) can be rewritten into a symbolic form

$$x_1 + x_2 \to (\lambda_1 + \lambda_2) + (\chi_1 + \chi_2). \quad (6)$$

This relation means that the λ-parts of the interacting constituents contribute to the production of the inclusive particle, while the χ-parts are responsible for the creation of its recoil. The maximum of the function (4) with the condition (3) can be obtained by searching for the unconstrained maximum of the function

$$F(y_a, y_b) \equiv \Omega\left(x_1(y_a, y_b), x_2(y_a, y_b), y_a, y_b\right) \quad (7)$$

of two independent variables y_a and y_b. There exists a single maximum of $F(y_a, y_b)$ for every momentum p in the allowable kinematical region. Values of y_a and y_b corresponding to this maximum have been determined numerically. Having obtained the fractions x_1, x_2, y_a, and y_b, we evaluate the function Ω according to (4). For fixed numbers δ and ϵ_F we obtain in this way the maximal value of Ω for every momentum p of the inclusive particle.

Since the momentum fractions are determined by means of the maximization of expression (4), they implicitly depend on δ and ϵ_F. The parameter ϵ_F enables to take effectively into account also prompt resonances out of which the inclusive particle of a given type may be created. At fixed mass parameter m_2, larger values of ϵ_F correspond to smaller y_a and y_b, which in turn give larger ratios m_2/y_b and m_1/y_a. In our phenomenological approach this means that production of the inclusive particle (m_1) and its counterpart (m_2) is a result of fragmentation from larger masses which mimic in a sense processes with prompt resonances. Values of these parameters are determined in accordance with the experiment and are discussed in the next sections.

2.2. Scaling Variable z and Scaling Function $\psi(z)$. The self-similarity of hadron interactions reflects a property that hadron constituents and their interactions are similar. This is connected with dropping of certain dimensional quantities out of the description of physical phenomena. The self-similar solutions are constructed in terms of the self-similarity parameters. We search for a solution

$$\psi(z) = \frac{1}{N\sigma_{\rm inel}}\frac{d\sigma}{dz} \tag{8}$$

depending on a single self-similarity variable z. Here $\sigma_{\rm inel}$ is an inelastic cross section of reaction (1) and N is an average particle multiplicity. The variable z depends on momenta and masses of the colliding and inclusive particles, structural parameters of the interacting objects, and dynamical characteristics of the produced system. We define the variable z as follows:

$$z = z_0\Omega^{-1}, \tag{9}$$

where

$$z_0 = \frac{\sqrt{s_\perp}}{(dN_{\rm ch}/d\eta|_0)^c m} \tag{10}$$

and Ω given by (4). For given reaction (1), the variable z is proportional to the transverse kinetic energy $\sqrt{s_\perp}$ of the constituent subprocess (2) consumed on the production of the inclusive particle (m_1) and its counterpart (m_2). The energy $\sqrt{s_\perp}$ is determined by the formula

$$\sqrt{s_\perp} = T_a + T_b, \tag{11}$$

where

$$\begin{aligned} T_a &= y_a(\sqrt{s_\lambda} - M_1\lambda_1 - M_2\lambda_2) - m_1, \\ T_b &= y_b(\sqrt{s_\chi} - M_1\chi_1 - M_2\chi_2) - m_2. \end{aligned} \tag{12}$$

The terms

$$\sqrt{s_\lambda} = [(\lambda_1 P_1 + \lambda_2 P_2)^2]^{1/2}, \quad \sqrt{s_\chi} = [(\chi_1 P_1 + \chi_2 P_2)^2]^{1/2} \tag{13}$$

represent the energy for production of the secondary objects moving in the scattered and recoil direction, respectively. The quantity $dN_{\rm ch}/d\eta|_0$ is the corresponding multiplicity density of charged particles in the central region of reaction (1) at pseudorapidity $\eta = 0$. The multiplicity density in the central interaction region is related to a state of the produced medium. The parameter c characterizes properties of this medium [6]. It is determined from multiplicity dependence of inclusive spectra. The mass constant m is arbitrary and we fix it at the value of nucleon mass.

The scaling function $\psi(z)$ is expressed in terms of the experimentally measured inclusive cross section $Ed^3\sigma/dp^3$, the multiplicity density $dN/d\eta$ at pseudorapidity η, and $\sigma_{\rm inel}$. Exploiting the definition (8) one can obtain the expression [6]

$$\psi(z) = -\frac{\pi s}{(dN/d\eta)\sigma_{\rm inel}} J^{-1} E\frac{d^3\sigma}{dp^3}, \tag{14}$$

where s is the square of the center-of-mass energy and J is the corresponding Jacobian. The multiplicity density $dN/d\eta$ in expression (14) concerns particular hadrons species. It depends on the center-of-mass energy, on various multiplicity selection criteria, and also on the production angles at which the inclusive spectra were measured. The procedure of obtaining the corresponding values of $dN/d\eta$ from the p_T spectra is described in Ref. [6]. The function $\psi(z)$ is normalized as follows:

$$\int_0^\infty \psi(z)dz = 1. \tag{15}$$

The above relation allows us to interpret the function $\psi(z)$ as a probability density to produce an inclusive particle with the corresponding value of the variable z.

3. PROPERTIES OF THE SCALING FUNCTION

Let us remind the properties of the z-presentation of experimental data already found in proton–(anti)proton collisions at high energies. These are the energy, angular, and multiplicity independence of the scaling function $\psi(z)$ for different types of hadrons, direct photons, and jets confirmed by numerous data obtained at ISR, $\mathrm{Sp\bar{p}S}$, Tevatron, and RHIC.

3.1. Energy Independence of $\psi(z)$. The energy independence of the z-presentation of inclusive spectra means that the shape of the scaling function is independent on the collision energy $\sqrt{s}$ over a wide range of the transverse momentum p_T of the inclusive particle. Results on the energy independence of the z-scaling for hadron production in proton–proton collisions were presented in Ref. [6]. The analyzed data [9–17] include negative pions, kaons, and antiprotons measured at FNAL, ISR, and RHIC energies. The spectra were measured over a wide transverse momentum range $p_T = 0.1 - 10$ GeV/c. The cross sections decrease from 10^2 to 10^{-10} mb/GeV^2 in this range. The strong dependence of the spectra on the collision energy increases with transverse momentum. The independence of the scaling function $\psi(z)$ on $\sqrt{s}$ was found for the constant values of the parameters $c = 0.25$ and $\delta = 0.5$ for all types of the analyzed hadrons ($\pi, K, \bar{p}$). The value of ϵ_F increases with the the mass of the produced hadron. None of these parameters depends on the kinematical variables. This was demonstrated for charged particles, negative pions, kaons, and antiprotons in the range of $\sqrt{s} = 19 - 200$ GeV. The z-presentation of particle spectra produced in proton–antiproton collisions was studied as well. In this case the energy independence of the scaling function was obtained for different set of parameters. The scaling functions for proton–(anti)proton collisions have similar shapes but differ in the region of large z. The different values of the slope parameter β ($\beta_{pp} > \beta_{p\bar{p}}$) of the scaling function, $\psi(z) \sim z^{-\beta}$, for charged hadron, direct photon, π^0 meson, and jet production in pp and $p\bar{p}$ collisions at high z were found in Ref. [18].

3.2. Angular Independence of $\psi(z)$. The angular independence of the z-presentation of inclusive spectra means that the shape of the scaling function is independent of the angle $\theta_{\rm cms}$ of the produced particles over a wide range of the transverse momentum p_T. Results on the angular properties of the z-scaling in proton–proton collisions are presented in Ref. [6]. The analyzed experimental data [19] on angular dependence of inclusive spectra include negative pions, kaons, and antiprotons measured at ISR energies. The angles cover the range $\theta_{\rm cms} = 3 - 90^\circ$. The central and fragmentation regions are distinguished by a different behavior of differential cross sections. The analysis included the transverse momentum spectra of charged hadrons for $\theta_{\rm cms} = 5$ and 13° [20] obtained by the BRAHMS Collaboration at RHIC. The data cover a wide range of the transverse momenta $p_T = 0.25 - 3.45$ GeV/c of the produced hadrons at the collision energy $\sqrt{s} = 200$ GeV. The angular independence of the scaling function $\psi(z)$ for charged particles, negative pions, kaons, and antiprotons was obtained for the same values of the parameters c, δ, and ϵ_F which give the energy independence of $\psi(z)$. This represents different values of ϵ_F for pions, kaons, antiprotons and the same values of δ and c for all of them. The scaling function is sensitive to the value of m_2 for small production angles $\theta_{\rm cms}$. This parameter was determined from the corresponding exclusive reactions at the kinematical limit (for

$x_1 = x_2 = y_a = y_b = 1$). Using Eq. (3), this gives $m_2 = m(\pi^+)$, $m_2 = m(K^+)$, and $m_2 = m(p)$, for the inclusive production of π^-, K^-, and antiprotons, respectively. Note that the charged hadron multiplicity density $dN_{\rm ch}/d\eta|_{\eta=0}$ represents an angular independent factor in the definition of the variable z which is the same for all particle species. On the contrary, the scaling function for pions, kaons, antiprotons is normalized (14) to the angular-dependent multiplicity density $dN/d\eta$ of the corresponding particles, respectively.

3.3. Multiplicity Independence of $\psi(z)$. The multiplicity independence of the z-presentation of inclusive spectra means that the shape of the scaling function $\psi(z)$ does not depend on the multiplicity selection criteria characterized by the different values of $dN_{\rm ch}/d\eta$. The multiplicity density influences the shape of the inclusive spectra especially at high transverse momenta [21]. At low p_T the dependence of the cross sections on $dN_{\rm ch}/d\eta$ concerns mainly the absolute values and much less the shape. Results on the multiplicity independence of the z-scaling in proton–proton collisions were presented in Ref. [6]. The analysis was performed using the K^0_S-meson and Λ-baryon spectra [22] obtained by the STAR Collaboration at $\sqrt{s} = 200$ GeV for different multiplicity classes. The charged multiplicity density was varied in the range $dN_{\rm ch}/d\eta = 1.3 - 9.0$. The transverse momentum distributions were measured in the central rapidity range $|\eta| < 0.5$ up to the momentum $p_T = 4.5$ GeV/c. The multiplicity independence of the scaling function provides a strong restriction on the parameter c. Both data favor the same value of $c = 0.25$ as was obtained from the energy independence of the z-scaling in proton–proton collisions. Similar applies to the p_T distributions of charged particles [21] associated with the different multiplicity criteria.

An analysis of the spectra of direct photons and jets gives somewhat different results in the sense, that the energy, angular, and multiplicity scaling were obtained by other set of the parameters c, δ, and ϵ_F. Nevertheless, the corresponding parameters do not depend on the kinematical variables, similarly as in the case of the z-scaling for identified hadrons produced in proton–(anti)proton collisions.

4. NEW PROPERTIES OF z-SCALING

In this section we study possibility of a unified description of the particle spectra of different hadrons using properties of their z-presentation. The analysis is based on the observation that simultaneous energy, angular, and multiplicity independence of the z-scaling for negative pions, kaons, and antiprotons produced in proton–proton collisions gives the same shape of the scaling function $\psi(z)$. This flavor independence of $\psi(z)$ is confirmed here for other inclusive particles including the particles with heavy quarks. The independence in proton–antiproton interactions is observed with the exception of large z, where the functions $\psi(z)$ for pp and $p\bar{p}$ collisions mutually differ. The transverse momentum spectra of

J/ψ [23] and Υ [24] mesons measured at the Tevatron energies $\sqrt{s} = 1800$ and 1960 GeV make it possible to investigate the behavior of the scaling function in the region of very small z (up to 10^{-3}). In this region we observe a saturation of $\psi(z)$ which can be approximated by a constant. The saturation and flavor independence of the scaling function for different hadrons with light and heavy quarks are confirmation of the factorization

$$\frac{d^2\sigma}{dzd\eta} = \psi(z)\frac{d\sigma}{d\eta} \tag{16}$$

of the inclusive cross sections. This property of the z-scaling is valid for pp collisions in a large range of kinematical variables. The factorization of the differential cross section in the variable z and the pseudorapidity η was demonstrated [6] as the angular independence of the z-scaling for $\theta_{\rm cms} = 3 - 90^\circ$. The scaling property at small angles gives strong restriction on the parameter m_2 which was found to be equal to the mass of the inclusive particle for the negative pions, kaons, and antiprotons. The same relation, $m_2 = m_1$, is used here for all types of the inclusive hadrons.

4.1. Flavor Independence of $\psi(z)$. Evidence of flavor independence of z-scaling was for the first time noted in Ref. [18]. It was found that the value of the slope parameter β of the scaling function $\psi(z)$ at high z is the same for different types of produced hadrons $(\pi, K, \bar{p})$. The hypothesis was later supported by the results of an analysis of hadron $(\pi^{\pm,0}, K, \bar{p})$ spectra for high p_T in pp and pA collisions. Here we show that flavor independence of the z-presentation of hadron spectra is valid for different hadrons over a wide range of the variable z. Hence we exploit the scaling transformation

$$z \to \alpha_F z, \quad \psi \to \alpha_F^{-1}\psi \tag{17}$$

for comparison of the shape of the scaling function $\psi(z)$ for different hadron species. The parameter α_F is a scale independent quantity. The transformation does not change the shape of $\psi(z)$. It preserves the normalization equation (15) and does not destroy the energy, angular, and multiplicity independence of the z-presentation of particle spectra.

Figure 2, *a* shows the z-presentation of the spectra of negative pions, kaons, antiprotons, and $\Lambda's$ produced in pp collisions over the range $\sqrt{s} = 19 - 200$ GeV and $\theta_{\rm cms} = 3 - 90^\circ$. The symbols represent data on differential cross sections measured in the central [9–11, 13, 15, 16, 25] and fragmentation [19] regions, respectively. The analysis comprises the inclusive spectra of particles [26, 27] measured up to very small transverse momenta ($p_T \simeq 45$ MeV/*c* for pions and $p_T \simeq 120$ MeV/*c* for kaons or antiprotons). One can see that the distributions of different hadrons are sufficiently well described by a single curve over a wide z-range $(0.01 - 30)$. The function $\psi(z)$ changes more than twelve orders of

magnitude. The solid lines represent the same curve shifted by multiplicative factors for reasons of clarity. The same holds for the corresponding data shown with the different symbols. The indicated values of the parameter ϵ_F ($\epsilon_\pi = 0.2, \epsilon_K \simeq 0.3, \epsilon_{\bar{p}} \simeq 0.35, \epsilon_\Lambda \simeq 0.4$) are consistent with the energy, angular, and multiplicity independence of the z-presentation of spectra for different hadrons. The parameters were found to be independent of kinematical variables ($\sqrt{s}, p_T$, and $\theta_{\rm cms}$). The scale factors α_F are constants which allow us to describe the z-presentation for different hadron species by a single curve. The estimated errors of α_F are at the level of 20%.

Figure 2, *b* shows similar results for other hadrons ($\rho, \omega, \phi, K^*, \Xi$) produced in pp collisions at $\sqrt{s} = 200$ GeV and $\theta_{\rm cms} = 90\,^\circ$. The experimental data [28–32] on inclusive spectra are compared with the pion distributions [15] measured at RHIC. The shape of $\psi(z)$ for these particles is described by the same curve (solid line) as depicted in Fig. 2, *a*. The black circle at the lowest $z \simeq 0.007$ corresponds to the STAR data [31] on K^* resonances measured in the region where the scaling function is saturated. Based on the obtained results we conclude that RHIC data on pp collisions confirm the flavor independence of the z-scaling including the production of particles with very small p_T.

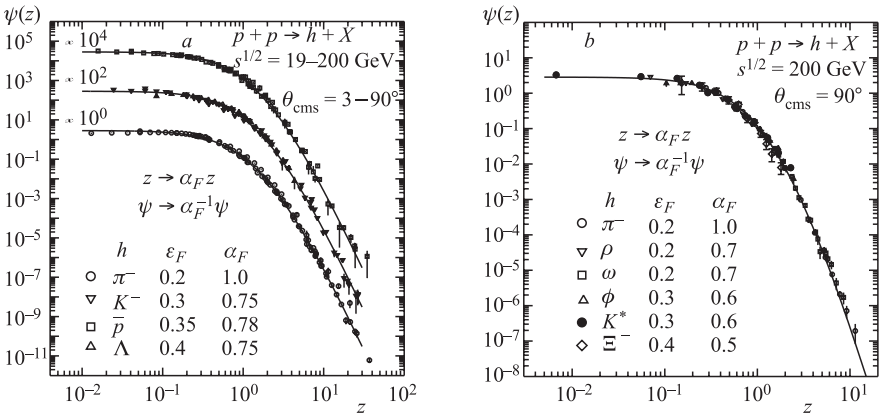

Fig. 2. The flavor independence of z-scaling. The spectra of π^-, K^-, $\bar{p}$, Λ (*a*) and ρ, ω, ϕ, K^*, Ξ (*b*) hadrons produced in pp collisions in z-presentation. Data are taken from Refs. [9–11, 13, 15, 16, 19, 25–32]. The solid line is obtained by fitting the data

The inclusive spectra of heavier hadrons ($J/\psi, D^0, B, \Upsilon$) [23,24,33] obtained at the Tevatron energies $\sqrt{s} = 1800$ and 1960 GeV allow us to verify the new property of the z-scaling in $p\bar{p}$-collisions. The data include measurements up to small transverse momenta ($p_T \simeq 125$ MeV/c for charmonia, $p_T \simeq 290$ MeV/c for bottomia, and $p_T \simeq 500$ MeV/c for B mesons). Figure 3, *a* shows the transverse

momentum spectra of $J/\psi, D^0, B$, and Υ mesons in the z-presentation. The scaling function is the same for hadrons with light and heavy flavors produced in pp and $p\bar{p}$ collisions in the range $z = 0.001 - 4$. This is indicated by the same line as in Fig. 2. The corresponding values of the parameters α_F and ϵ_F are found to be $\alpha_{J/\psi} = 0.23$, $\alpha_{D^0} \simeq 0.23$, $\alpha_B \simeq 0.12$, $\alpha_{\Upsilon(1S)} \simeq 0.15$ and $\epsilon_{J/\psi} = 1.0$, $\epsilon_{D^0} \simeq 0.4$, $\epsilon_B \simeq 0.4$, $\epsilon_{\Upsilon(1S)} \simeq 0.4$, respectively. Figure 3, *b* demonstrates results of combined analysis of the RHIC [34] and Tevatron [23] data on J/ψ-meson spectra measured in pp and $p\bar{p}$ collisions at different energies $\sqrt{s} = 200, 1800, 1960$ GeV and angles $\theta_{\rm cms} = 22, 90^\circ$ in the z-presentation. The solid line is the same one as shown in Figs. 2 and 3, *a*.

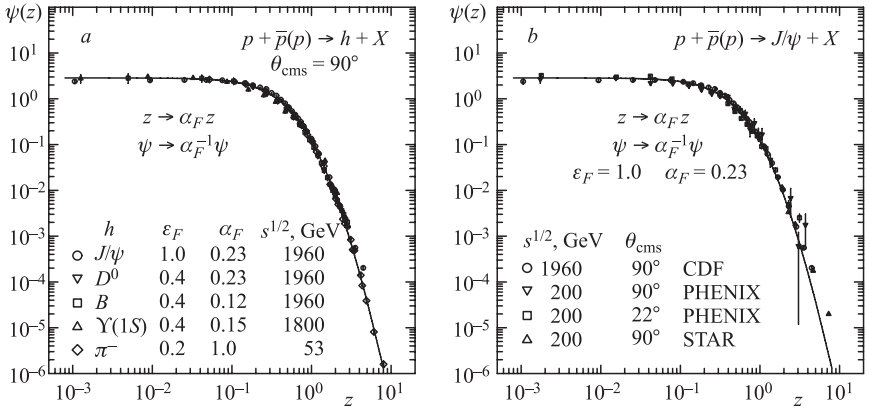

Fig. 3. The flavor independence of z-scaling. The spectra of $J/\psi, D^0, B, \Upsilon, \pi^-$ (*a*) and J/ψ (*b*) mesons produced in $pp/p\bar{p}$ collisions in z-presentation. Data are taken from Refs. [23, 24, 33, 34]. The solid line is the same as in Fig. 2

From the performed analysis we conclude that ISR, RHIC, and Tevatron data on inclusive spectra manifest the flavor independence of the scaling function $\psi(z)$ over a wide range of z. We would like to stress that the obtained result is based on p_T distributions of the cross sections $Ed^3\sigma/dp^3$ which reveal strong dependence on the energy, angle, multiplicity, and type of the produced particle.

4.2. Saturation of $\psi(z)$. The description of particle spectra in terms of the variable z depends on the parameters $\delta_{1,2}, \epsilon_F$, and c. In the region of high z, the production of different hadrons is characterized by different values of ϵ_F. A reliable estimation of this parameter requires processes with high p_T. The same applies to $\delta_{1,2}$ which relates to the structure of the colliding particles in the initial state. On the contrary, the low-z region corresponds to the small values of p_T and low momentum fractions x_1, x_2, y_a, and y_b. In this region z tends to zero as p_T decreases or $\sqrt{s}$ increases. Here is $\Omega \simeq 1$ and the scaling variable can

be approximated by $z \sim s_{\perp}^{1/2}/(dN_{\rm ch}/d\eta|_0)^c$. The behavior of $\psi(z)$ at low z is therefore governed by the single parameter c.

As is seen from Figs. 2 and 3, the z-presentation of hadron distributions demonstrates weak dependence on the variable z in the soft (low p_T) region. The data on the pion, kaon, antiproton and especially on J/ψ and Υ spectra manifest saturation in the range $z = 10^{-3} - 10^{-1}$. This regime is characterized by an approximate constant behavior of the scaling function, $\psi(z) \simeq {\rm const}$. The similar dependence is observed for other hadrons (K^*, B, ρ,...) at low p_T. A characteristic of the saturation is the slope β of the scaling function which is diminishing with the decreasing z. The value of β is approximately zero for $z = 10^{-3} - 10^{-1}$.

One can assume that the asymptotic behavior of $\psi(z)$ at $z \to 0$ is universal and reflects properties of the produced system consisting of its constituents (hadrons or quark and gluons). The universal scaling behavior in this region suggests that mechanism of particle production at low p_T is governed by soft self-similar processes which reveal some kind of a mutual equilibrium leading to the observed saturation.

5. A MICROSCOPIC PICTURE OF CONSTITUENT SUBPROCESSES

The approach based on the z-scaling concept allows us to develop a microscopic scenario of particle production in terms of the constituent interactions. Here we discuss some features of this scenario. We attribute the quantity z to any inclusive particle in reaction (1). The scaling variable z has character of a fractal measure. It consists of the finite part z_0 and of the divergent factor Ω^{-1}. The factor Ω^{-1} describes a resolution at which an underlying subprocess can be singled out of the inclusive reaction (1). The $\Omega(x_1, x_2, y_a, y_b)$ is proportional to number of all configurations containing the incoming constituents which carry the fractions x_1 and x_2 of the momenta P_1 and P_2 and which fragment to the inclusive particle (m_1) and its counterpart (m_2) with the corresponding momentum fractions y_a and y_b. The parameters δ_1 and δ_2 have relation to fractal structure of the colliding objects (hadrons or nuclei). They are interpreted as fractal dimensions of the colliding objects in the space of the momentum fractions. The parameters ϵ_a and ϵ_b characterize the fractal behavior of the fragmentation process in the final state. A common property of fractal measures is their divergence with the increasing resolution. The scaling variable has this property as the resolution Ω^{-1} goes to infinity,

$$z(\Omega) \to \infty, \quad \text{if} \quad \Omega^{-1} \to \infty. \tag{18}$$

It means that z is the scale-dependent quantity. For an infinite resolution the whole reaction (1) degenerates to a single subprocess (2), all momentum fractions

become unity ($x_1 = x_2 = y_a = y_b = 1$) and $\Omega = 0$. This kinematical limit corresponds to the fractal limit $z = \infty$. In the general case, the momentum fractions are determined from a principle of a minimal resolution of the fractal measure z. The principle states that the resolution Ω^{-1} should be minimal with respect to all binary subprocesses (2) in which the inclusive particle m_1 with the momentum p can be produced. It fixes the values of the corresponding momentum fractions x_1, x_2, y_a, and y_b and singles out the most effective binary subprocess which underlies the inclusive reaction (1).

5.1. Momentum Fractions versus p_T and $\sqrt{s}$. The method of determination of the momentum fractions makes it possible to analyze kinematics of the constituent interactions in the framework of the developed approach. The study of $x_1 - x_2$ and $y_a - y_b$ correlations and their dependences on the collision energy and transverse momentum of the inclusive particle gives us the possibility to look at the microscopic picture of the underlaying subprocesses.

The fractions x_1 and x_2 characterize amount of the energy (momentum) of the interacting protons (antiprotons) carried by their constituents which undergo the binary collision (2) that underlies the inclusive reaction (1). Figure 4, *a* shows the dependence of the fraction x_1 on the transverse momentum p_T of the negative pions, kaons, and antiprotons produced in pp collisions at $\sqrt{s} = 19, 53, 200$ GeV and $\theta_{\rm cms} = 90\,^\circ$. The fractions x_1 and x_2 are equal to each other in that case. They increase nearly linearly with the transverse momentum p_T. For fixed p_T, the fraction x_1 decreases as the collision energy $\sqrt{s}$ increases. The x_1 is larger for the production of heavy particles as compared with light ones. The kinematical limit of reaction (1) corresponds to $x_1 = x_2 = 1$ at any collision energy and for any type of the inclusive particle. This can be seen in Fig. 4, *a* for $\sqrt{s} = 19$ GeV where the fraction x_1 approximates unity at $p_T \simeq 9$ GeV/*c* for all three particles.

The correlation $x_1 - x_2$ for the π^-, K^-, and $\bar{p}$ production at the energy $\sqrt{s} = 53$ GeV and for various detection angles is shown in Fig. 4, *b*. The central ($\theta_{\rm cms} = 90, 58, 40\,^\circ$) and fragmentation ($\theta_{\rm cms} = 2.86\,^\circ$) regions are distinguished by a different mutual behavior of x_1 and x_2. The $x_1 - x_2$ correlation at $\theta_{\rm cms} = 90\,^\circ$ is depicted as a strait line. For other angles belonging to the central interaction region, the correlation becomes more complicated and depends on the particle type. Both tendencies diminish with the increasing p_T where the fraction x_2 demonstrates linear dependence on x_1 over a wide range. This is a common feature for all hadron species. The situation is different in the fragmentation region. The fraction x_2 is much less than x_1 and strongly depends on the type of the inclusive particle at the small angle $\theta_{\rm cms} = 2.86\,^\circ$. The heavier particle the larger x_2. The increase of x_2 with x_1 is very slow in the range of small angles. This is changed dramatically near the kinematical limit ($x_1 \simeq 1$) where the fraction x_2 begins to grow larger.

The dependence of the momentum fractions y_a and y_b on the kinematical variables $(p_T, \theta_{\rm cms}, \sqrt{s})$ describes features of the fragmentation process. The

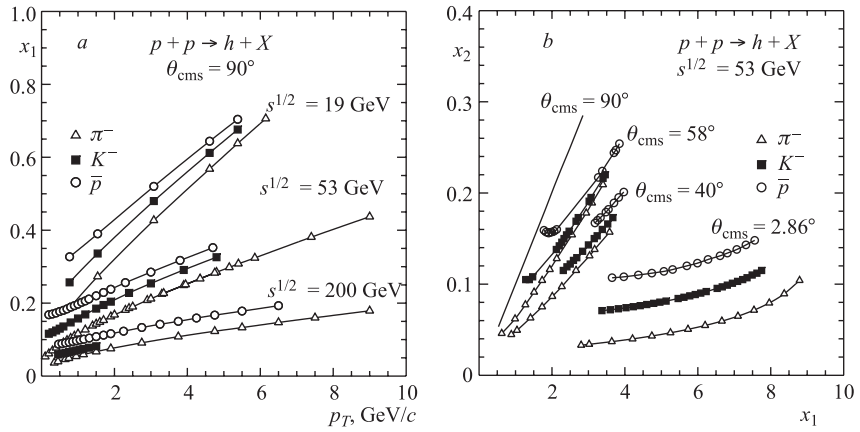

Fig. 4. *a*) The dependence of the fraction x_1 on the transverse momentum p_T at $\theta_{\rm cms} = 90^\circ$. *b*) The correlation between the fractions x_1 and x_2 at $\sqrt{s} = 53$ GeV in the central and fragmentation regions

fraction y_a characterizes dissipation of the energy and momentum of the object produced by the underlying constituent interaction into the near side of the inclusive particle. This effectively includes energy losses of the scattered secondary partons moving in the direction of the registered particle as well as feed down processes from prompt resonances out of which the inclusive particle may be created. The fraction y_b governs the recoil mass in the constituent subprocess. Its value characterizes the dissipation of the energy and momentum in the away side direction of the inclusive particle.

Figure 5, *a* shows the dependence of y_a on the transverse momentum p_T for the negative pions, kaons, and antiprotons produced in pp collisions at the energies $\sqrt{s} = 19, 53, 200$ GeV and $\theta_{\rm cms} = 90^\circ$. All curves demonstrate a nonlinear monotonic growth with p_T. It means that the energy dissipation associated with the production of a high-p_T particle is smaller than for the inclusive processes with lower transverse momenta. This feature is similar for all inclusive reactions at all energies. Decrease of the fractions y_a with the increasing collision energy is another property of the considered mechanism. It corresponds to more energy dissipation at higher energies. This can be due to the larger energy losses and/or due to the heavy prompt resonances. The third characteristic is a slight decrease of y_a with the mass of the inclusive particle. It implies more energy dissipation for creation of heavier hadrons as compared with hadrons with smaller masses. The asymptotic value of $y_a = 1$ is reached at the kinematical limit for all particle species.

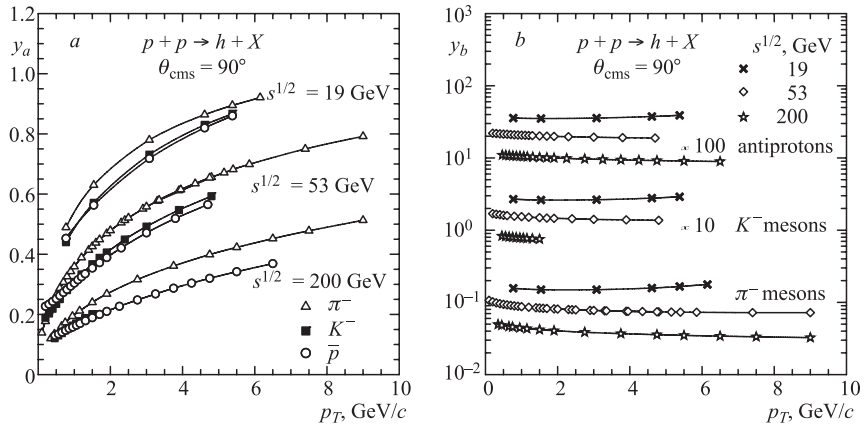

Fig. 5. The dependence of the fractions y_a (a) and y_b (b) on the transverse momentum p_T for π^-, K^-, and $\bar{p}$ produced in the pp collisions at $\sqrt{s} = 19, 53$, and 200 GeV in the central rapidity region

The dependence of y_b on p_T reflects kinematical properties of the recoil system. One can see from Fig. 5, b that y_b is nearly independent of p_T. It is smaller than y_a and decreases with the increasing collision energy $\sqrt{s}$. The values of y_b are larger for particles with higher masses. The qualitative properties of the p_T dependence of y_b are similar for different hadrons. The small values of y_a mean that the momentum balance in the production of an inclusive particle from a subprocess is more likely compensated with many particles with smaller momenta than by a single particle with a higher momentum moving in the opposite direction.

The p_T-dependence of y_a and y_b for other hadrons produced in pp collisions have similar behavior. This is demonstrated in Fig. 6, a on the data [15,16,25,28–32] at $\sqrt{s} = 200$ GeV and $\theta_{\rm cms} = 90^\circ$ obtained at RHIC. The hollow symbols demonstrate growth of y_a with p_T. The full symbols show flattening of y_b in the range of $p_T = 0.2 - 10$ GeV/c. Note that both fractions become equal to each other, $y_a \simeq y_b$, for heavier particles and low transverse momenta. This together with $m_1 = m_2$ means that, at low p_T, the objects produced in the constituent collision into the near- and away-side direction have equal masses. The feature is even more pronounced for particles with heavy quarks. It is well seen from Fig. 6, b where the momentum dependence of y_a and y_b is demonstrated for $J/\psi, D^0, B$, and Υ mesons produced in $p\bar{p}$ collisions at the Tevaron energies $\sqrt{s} = 1800$ and 1960 GeV. The spectra correspond to the central rapidity range. The p_T-dependence of y_a and y_b has similar behavior as for data obtained at the RHIC energy.

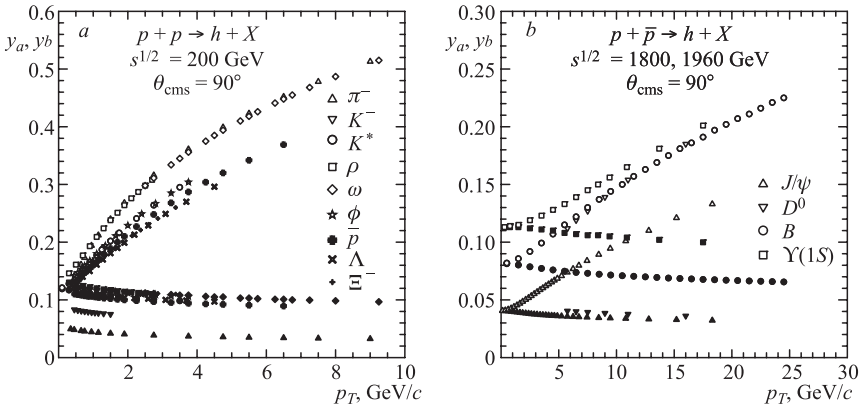

Fig. 6. The dependence of the fractions y_a and y_b on the transverse momentum p_T for: *a*) π^-, K^-, K^*, ρ, ω, ϕ, $\bar{p}$, Λ, Ξ^- hadrons produced in pp collisions at $\sqrt{s} = 200$ GeV and *b*) J/ψ, D^0, B, $\Upsilon(1S)$ mesons produced in $\bar{p}p$ collisions at $\sqrt{s} = 1800, 1960$ GeV

There is, however, a particularity in the absolute values of the momentum fractions which concern the J/ψ-meson production. The corresponding curves for y_a and y_b lay much below than what one could expect when compared with other particles, even at high p_T. This is a consequence of the relatively large value of $\epsilon_{J/\psi} = 1$ which follows from the requirement of the energy independence of $\psi(z)$ for the charmonium production (see Fig. 3). In our approach it means that J/ψ meson is produced from larger masses accompanied with extra large dissipation of energy in the final state. This exceptional property predestinate the J/ψ meson to be a suitable probe in AA collisions where the energy losses can be sensitive to different phases of the created matter.

A comparison of the momentum fractions y_a and y_b for the charmonium production in pp [34] and $p\bar{p}$ [23] collisions at $\sqrt{s} = 200$ and 1960 GeV is shown in Fig. 7, *a*. The fractions follow the general trend, i.e., a decrease with the collisions energy, growth of y_a, and approximate constancy of y_b with p_T. The equality of both fractions at low p_T remains preserved independent on $\sqrt{s}$. Another feature typical for all types of the inclusive particles is the angular dependence of the fractions. The y_a increases significantly with the decreasing angle $\theta_{\rm cms}$. It means that the energy dissipation from the constituent subprocess is much smaller in the fragmentation region as compared to the central interaction region. The change of the fraction y_b with the angle $\theta_{\rm cms}$ is small. A levelling of y_b with p_T for small angles is observed.

The sensitivity of the transverse momentum dependence of y_a and y_b to the mass of the Υ states $(1S, 2S, 3S)$ is demonstrated in Fig. 7, *b*. The symbols correspond to the experimental data [24,35] on cross sections measured at FNAL.

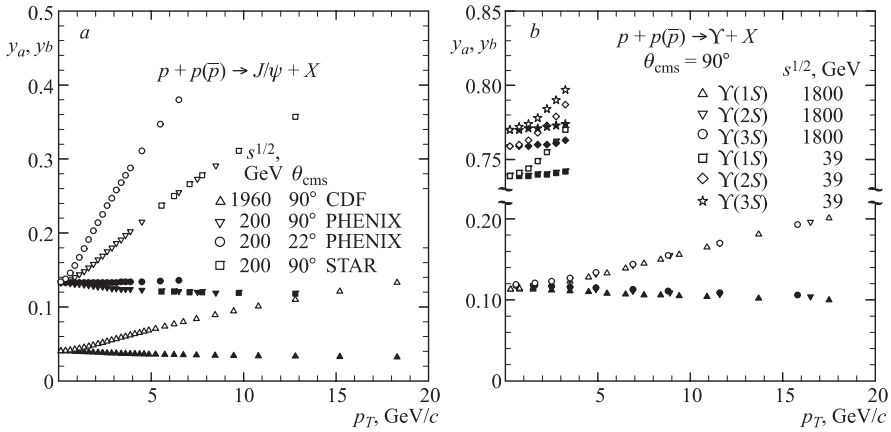

Fig. 7. The dependence of the fractions y_a and y_b on the transverse momentum for J/ψ (a) and Υ (b) mesons produced in pp and $\bar{p}p$ collisions at $\sqrt{s} = 200$, 1960 GeV and 39, 1800 GeV, respectively

It turns out that the momentum fractions change visibly with the respective state of the bottomium at smaller collision energy. The heavier mass the larger fractions. This is connected with different energy losses which seem to depend on the mass state of the Υ meson at this energy. At higher energies the momentum fractions become insensitive to the single states of this particle. The curves for the $1S$, $2S$, and $3S$ states coincide each other at $\sqrt{s} = 1800$ GeV in the momentum range $p_T = 0.5 - 17$ GeV/c.

5.2. Recoil Mass M_X versus p_T and $\sqrt{s}$. Another characteristic of the constituent interactions is the recoil mass

$$M_X = x_1 M_1 + x_2 M_2 + m_2/y_b \tag{19}$$

released in the underlying subprocess (2). It is defined by the right-hand side of Eq. (3). The quantity is proportional to the momentum fractions x_1 and x_2 of the interacting objects with the masses M_1 and M_2. Its relation to the fractions y_a and y_b is given by the simple dependencies $x_{1,2} = x_{1,2}(y_a, y_b)$ listed in Ref. [6].

The method of determination of y_a and y_b makes them implicitly-dependent on δ and ϵ_F. These parameters are obtained from the z-scaling approach to analysis of experimental data on inclusive particle distributions. In such a way the recoil mass M_X has an internal connection to the structure of the colliding objects, constituent interactions, and process of formation of the individual hadrons. In the very vicinity of the kinematical limit, the recoil mass is kinematically bounded to approximate the value $M_1 + M_2 + m_2$.

Figure 8, *a* shows the dependence of the recoil mass on the transverse momenta of the negative pions, kaons, and antiprotons produced in pp collisions at the energis $\sqrt{s} = 19, 53$, and 200 GeV in the central rapidity region. For the sake of clarity, the values of M_X are presented on a log-scale with the multiplication factors 10 and 100 for K^- and $\bar{p}$, respectively. All curves demonstrate small growth at low p_T followed by a successive flattening. They reveal a characteristic increase with the collision energy and mass of the inclusive particle. The similar dependencies of M_X on p_T for other hadrons measured at the RHIC energy $\sqrt{s} = 200$ GeV are presented in Fig. 8, *b*. The data correspond to the central interaction region. The dependence of M_X on p_T for $J/\psi, D^0, B$, and Υ meson production in $p\bar{p}$-collisions at the Tevatron energies $\sqrt{s} = 1800$ and 1960 GeV is presented in Fig. 9, *a*.

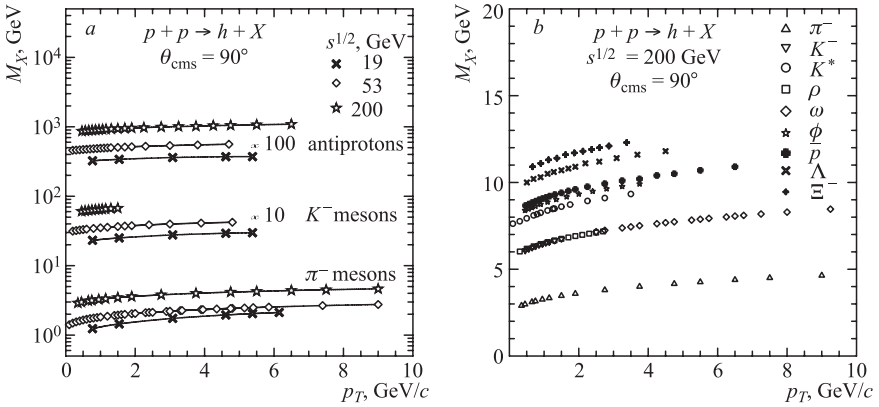

Fig. 8. The recoil mass M_X in the constituent subprocess underlying the hadron production in pp collisions at $\sqrt{s} = 19, 53$, and 200 GeV in dependence on the transverse momentum p_T

We would like to draw attention to the large recoil mass for the J/ψ-meson production. It is approximately equal to the values of M_X for the Υ mesons with a small exception at low transverse momenta (p_T below 7 GeV/c). The mass increases with p_T and reaches the value of 95 GeV at $p_T = 18$ GeV/c. The curves for B and D^0 mesons lay considerably below. The extra large values of the recoil mass in the charmonium production is connected with the abnormal small values of the corresponding momentum fractions y_a and y_b (see discussion to Fig. 6, *b*). A comparison of the momentum dependence of M_X for J/ψ meson at $\sqrt{s} = 200$ and 1960 GeV is shown in Fig. 9, *b*. Here one can see the strong sensitivity of the recoil mass to the collision energy $\sqrt{s}$. Its angular dependence

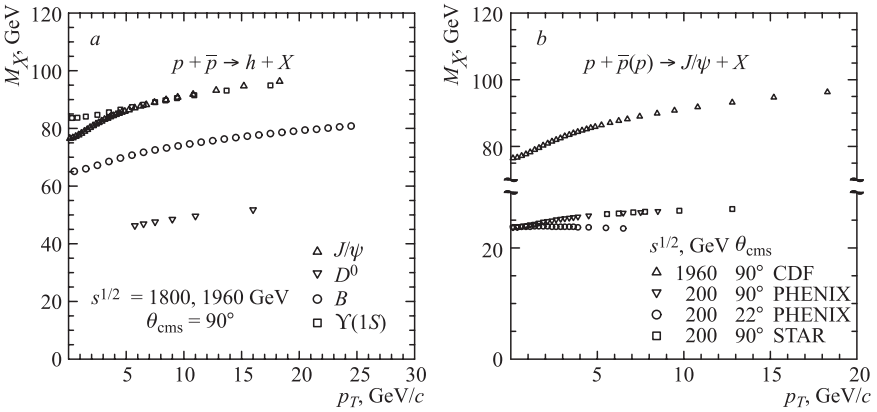

Fig. 9. The recoil mass M_X in the constituent subprocess underlying production of: *a*) J/ψ, D^0, B, $\Upsilon(1S)$ mesons in $p\bar{p}$ collisions at $\sqrt{s} = 1800$, 1960 GeV and *b*) J/ψ mesons in $pp/p\bar{p}$ collisions at $\sqrt{s} = 200$, 1960 GeV in dependence on the transverse momentum p_T

at $\sqrt{s} = 200$ GeV is rather weak. The approximate constancy of M_X at the angle $\theta_{\rm cms} = 22^\circ$ corresponds to the levelling of the fraction y_b with p_T shown in Fig. 7, *a*.

6. DISCUSSION

An analysis of ISR, RHIC, and Tevatron experimental data on inclusive cross sections for different hadron species performed in z-presentation shows the flavor independence of the shape of the scaling function $\psi(z)$. This was demonstrated over a wide range of the kinematical variables for proton–proton and proton–antiproton collisions. A saturation of $\psi(z)$ was found in the region $z < 10^{-1}$ for hadrons with light and heavy quarks. The data on J/ψ- and Υ-meson production confirm the saturation up to very small values of $z \simeq 10^{-3}$. The observed universality is a manifestation of the self-similarity of particle production at a constituent level. The dynamical behavior of the interacting system revealed in the distributions of the inclusive particles is described by the function $\psi(z)$ which demonstrates flattening in the experimentally achievable low-z region (Figs. 2 and 3). The slope $\beta(z)$ of the scaling function diminishes with the decreasing z and becomes zero when the scaling function flattens out. It was found that for both asymptotic regimes, at low and high z, the interacting system is characterized by the equation

$$\frac{d\ln\psi(z)}{d\ln z} = \text{const}. \tag{20}$$

The obtained results give strong support that flavor independence of $\psi(z)$ for variety of light and heavy hadrons and its behavior (20) at both asymptotic limits reflect general trend of hadron production in the high energy proton–proton and proton–antiproton collisions over a wide range of transverse momenta.

6.1. Variable z and Entropy. In this part we discuss analogy between the parameters used in the z-scaling concept and some thermodynamical quantities (entropy, specific heat, chemical potential) of a multiple particle system. There exists a connection between the variable z and entropy. The scaling variable is proportional to the ratio

$$z \sim \frac{\sqrt{s_\perp}}{W} \tag{21}$$

of the transverse kinetic energy $\sqrt{s_\perp}$ and the maximal value of the function

$$W(x_1, x_2, y_a, y_b) = (dN_{\rm ch}/d\eta|_0)^c \ \Omega(x_1, x_2, y_a, y_b) \tag{22}$$

in the space of the momentum fractions. The quantity W is proportional to all parton and hadron configurations of the colliding system which can contribute to the production of the inclusive particle with the momentum p. According to statistical physics, entropy of a system is given by a number of its statistical states as follows:

$$S = \ln W. \tag{23}$$

The most likely microscopic configuration of the system is given by the maximal value of S. In our approach, the configurations comprise all mutually independent constituent subprocesses (2). The corresponding subprocesses which can contribute to the production of the inclusive particle with the 4-momentum p are considered as subject to the condition (3). The underlying subprocess, in terms of which the variable z is determined, is singled out from the corresponding subprocesses by the principle of maximal entropy S.

In thermodynamics, entropy for an ideal gas is determined by the formula

$$S = c_V \ln T + R \ln V + S_0, \tag{24}$$

where c_V is a specific heat and R is a universal constant. The temperature T and the volume V characterize a state of the system. Using (22) and (23), we can write the relation

$$S = c \ \ln [dN_{\rm ch}/d\eta|_0] + \ln [(1-x_1)^{\delta_1}(1-x_2)^{\delta_2}(1-y_a)^{\epsilon_a}(1-y_b)^{\epsilon_b}]. \tag{25}$$

Next we exploit analogy between (24) and (25). The analogy is supported by the plausible idea that interaction of the extended objects like hadrons and nuclei can be treated at high energies as a set of independent collisions of their constituents. Such a concept justifies a division of the system into the part comprising the

selected subprocess which underlies production of the inclusive particle and the rest of the system containing all remaining microscopic configurations which lead to the produced multiplicity. The entropy (25) refers to the rest of the system. The multiplicity density $dN_{\rm ch}/d\eta|_0$ of particles in the central interaction region characterizes a «temperature» created in the system [36]. Provided that the system is in a local equilibrium, there exists a simple relation $dN_{\rm ch}/d\eta|_0 \sim T^3$ for high temperatures and small chemical potentials. Using the mentioned analogy, the parameter c plays a role of a «specific heat» of the produced matter. The second term in (25) depends on the volume of the rest of the system in the space of the momentum fractions $\{x_1, x_2, y_a, y_b\}$. The volume is a product of the complements of the fractions with the exponents which are generally fractional numbers, $V = l_1^{\delta_1} l_2^{\delta_2} l_3^{\epsilon_a} l_4^{\epsilon_b}$. This analogy emphasizes once more the interpretation of the parameters δ_1, δ_2, ϵ_a, and ϵ_b as fractal dimensions. In accordance with common arguments, the entropy (25) increases with the multiplicity density and decreases with the increasing resolution Ω^{-1}. In the considered analogy, the principle of a minimal resolution Ω^{-1} with respect to all subprocesses satisfying the condition (3) is equivalent to the principle of a maximal entropy S of the rest of the colliding system.

The entropy is determined up to an arbitrary constant $S_0 = \ln W_0$. Dimensional units entering the definition of the entropy can be included within this constant. In particular, it allows us to account for a relation between the dimensionless multiplicity density $dN_{\rm ch}/d\eta|_0$ and the temperature T. This degree of freedom is related to the transformation

$$z \to W_0 z, \quad \psi \to W_0^{-1}\psi. \tag{26}$$

In such a way the scaling variable and the scaling function are determined up to an arbitrary multiplicative constant. The constant W_0 is related to an absolute number of the microscopic states of the system. Its value is restricted by the positiveness of the entropy above some scale characterized by a maximal resolution Ω^{-1}. For the resolution corresponding to the fractal limit, W_0 is infinity. Thus, the transformation (26) is connected with a renormalization of the fractal measure z in agreement with its physical interpretation (21). The renormalization represents a shift of the entropy by the corresponding constant,

$$S = \ln W + \ln W_0. \tag{27}$$

6.2. Chemical Potential and Phase Space Occupancy. Let us consider a system where the number of particles can change. According to the first law of thermodynamics the internal energy U of such a system can be expressed as follows:

$$dU = TdS - pdV + \sigma_a dN_a + \sigma_{\bar{a}} dN_{\bar{a}}. \tag{28}$$

This shows how U depends on independent variations of the entropy S, volume V, and number of particles (antiparticles) $N_a, (N_{\bar{a}})$. The parameters T and p are the temperature and pressure of the system. The potentials σ_a and $\sigma_{\bar{a}}$ consist of two parts [37]

$$\sigma_a \equiv \mu_a + T \ln(\gamma_a), \tag{29}$$

which are expressed via the chemical potentials $\mu_a = -\mu_{\bar{a}}$ and the phase space occupancy $\gamma_a = \gamma_{\bar{a}}$ of the system constituents. First one controls the net number of particles $(N_a - N_{\bar{a}})$ arising from the particle and antiparticle difference. Second term regulates the number of particle–antiparticle pairs $(N_a + N_{\bar{a}})$. In statistical hadro-chemistry the factors are related to the relative and absolute chemical equilibrium, respectively [37]. The chemical potentials determine the statistical parameter Υ_a known as fugacity

$$\Upsilon_a = \exp(\sigma_a/T) = \gamma_a \exp(\mu_a/T), \tag{30}$$

which governs the yield of a corresponding particle type.

As shown in Sec. 4, the scaling functions of different hadrons coincide each other when applying the transformation (17) with the appropriate values of α_F. The coefficient α_F is ratio of the constants W_0 (27) for single hadrons. In principle, these properties can be used for estimation of the ratios of the corresponding phase space occupancy parameters γ_a. In Boltzmann approximation, the hadron yields are proportional to the chemical fugacities. If one assumes that at sufficiently high energy the chemical potentials μ_a become negligible on the right-hand side of (29), then it is possible to write

$$\gamma_1/\gamma_2 = \alpha_{F_1}/\alpha_{F_2}. \tag{31}$$

The ratio describes the relative yields of hadron pairs with the flavors F_1 and F_2. Exploiting the connection between the temperature T and the multiplicity density $dN/d\eta|_0$ discussed after Eq. (25), we can rewrite the relation (29) into the form

$$\sigma_{F_1} = \sigma_{F_2} + g(dN_{\rm ch}/d\eta|_0)^{1/3} \ln(\alpha_{F_1}/\alpha_{F_2}). \tag{32}$$

Here g is a constant which does not depend on the particle type. Knowing the values of α_F for different hadrons (they are quoted in Figs. 2 and 3 relative to π^- mesons with $\alpha_\pi = 1$), one can obtain a hierarchy of the potentials σ_F for the individual hadron species. A systematic analysis of α_F for mesons and baryons, its dependence on the mass, flavor content, and spin requires further, more detailed study.

6.3. z-Scaling and Phase Transitions. The self-similarity of the particle formation at low transverse momenta is a new specific feature which can give information on thermodynamical characteristics of the colliding system and clarify

its behavior. For sufficiently low p_T the scaling variable becomes resolution-independent function of the multiplicity density $dN_{\rm ch}/d\eta$ and the parameter c. Both quantities characterize medium produced in the high energy collisions. The multiplicity density of particles in the central interaction region can be connected with a «temperature» of the colliding system. The parameter c is interpreted as a «specific heat» of the produced medium. Its value $c = 0.25$ was found to be the same for different types of the inclusive hadrons. The estimated error is at the level of 10%. We expect that this parameter should change in consequence of a phase transition in the produced medium. The increase of the multiplicity (or energy) density should affect the medium characteristics in that case. A possible violation of the z-scaling in the low-z region connected with a change of the «specific heat» c might be considered as a manifestation of such a phase transition. Measurements of the cross sections for hadrons with heavy quarks at higher energies allow one to reach even lower values of z where the saturation of $\psi(z)$ could in principle change. We expect that such a change of the observed behavior of the scaling function could give indications on new physical effects in this region.

There are quantities in thermodynamics which are sensitive to phase transitions. A discontinuity of specific heat, compressibility factor and coefficient of thermal expansion characterizes second order phase transition of the thermodynamic system. The second derivative of the chemical potential

$$\partial^2\sigma/\partial T^2|_P = -c_P/T \tag{33}$$

is connected with a discontinuity of the specific heat in such a case. The quantities c in (25) and σ_F in (32) signify a specific heat and chemical potential, respectively. Their potential dependence on multiplicity density can be studied from suitable experimental data. A discontinuity of c associated with a jump in the second derivative of σ_F, especially at high $dN_{\rm ch}/d\eta|_0$, could be considered as a signature of the second-order phase transition in the medium produced in high energy hadron collisions.

It is usually assumed that bulk of the produced matter at low p_T (low z) consists of multitude of the strongly interacting constituents. There is no direct information on the type of the constituents. Even at high collision energies $\sqrt{s}$, the single constituent processes at low transverse momenta are experimentally invisible. Only indirect signatures can reveal the nature of the constituents. We suggest to use the analogs of the thermodynamical quantities such as the specific heat and chemical potentials which can be useful in the description of the produced matter. These quantities can be sensitive to phase transitions in the multiple particle systems.

According to the phase transition theory and theory of the critical phenomena, an abrupt change in the specific capacity, coefficient of thermal expansion and

compressibility with a small change in temperature near to a critical point is typical for the second-order phase transition [38–40]. The second-order phase transitions have a discontinuity in the first derivative of the entropy

$$c_V = \partial S/\partial \ln(T)|_V. \tag{34}$$

In our case, such a signature would correspond to a discontinuity or sharp growth of the parameter c near some critical point z_c. One can speculate that the value of c should become dependent on the transverse momentum p_T and rise sharply enough with the multiplicity density at low p_T. It is usually considered that the increase of the multiplicity density is connected with a growth of the energy density. Existence of the internal structure of the constituents would allow to store the energy into their internal degrees of freedom which is connected with a rise of the specific heat. We consider therefore that study of the inclusive cross sections of hadron production in the low-p_T region at high multiplicity densities $dN_{\rm ch}/d\eta$ and collision energies $\sqrt{s}$ is most preferable in searching for signatures of phase transitions in hadron matter.

7. CONCLUSIONS

Here we summarize the main results obtained in the paper. New properties of the z-scaling — the flavor independence and the saturation of $\psi(z)$ at low z — were established. We have studied the spectra of the inclusive particles produced in proton–proton and proton–antiproton collisions in z-presentation. The experimental data on inclusive cross sections of different hadrons obtained at ISR, RHIC, and Tevatron were used in the present analysis. The data cover a wide range of the collision energies $\sqrt{s} = 19 - 1960$ GeV, the transverse momenta $p_T = 0.1 - 10$ GeV/c, and the production angles $\theta_{\rm cms} = 3 - 90^\circ$. The variable z depends on the parameters δ, ϵ_F, and c. The parameters δ and ϵ_F characterize structure of the colliding (anti)protons and fragmentation process in the final state, respectively. Their values are fixed by the energy, angular, and multiplicity independence of $\psi(z)$ in the high-p_T part of the spectra. The third parameter c is interpreted as «specific heat» of the produced medium. The z-scaling is consistent with $c = 0.25$ and $\delta = 0.5$ for all types of the analyzed inclusive hadrons. The value of ϵ_F increases with the mass of the produced hadron. Estimated errors of the determination of the parameters do not exceed 10%. It was found that the parameters are independent of kinematical variables.

It was shown that renormalization of the scaling variable z allows one to reduce the scaling function of different hadrons to a single curve. The scaling function $\psi(z)$ was established to be flavor independent in a vide range of z. It means that the shape of $\psi(z)$ is the same for different hadrons in this region. This includes hadrons with light and heavy quarks produced in high energy pp

and $p\bar{p}$ collisions. A saturation regime of the function $\psi(z)$ was observed for $z < 0.1$. The approximate constancy of $\psi(z)$ was demonstrated up to $z \sim 10^{-3}$ for charmonia and bottomia. We conclude that a violation of the asymptotic behavior of the scaling function in the region of low z could give information on a phase transition of the produced matter. This should apply especially for the events with high multiplicity densities in both $pp/p\bar{p}$ and AA collisions at high energies.

A connection between the ingredients of the variable z allowing thermodynamical interpretation and the thermodynamical quantities (entropy, temperature, specific heat, chemical potential) characterizing multiparticle systems was discussed. The «specific heat» c was suggested as a parameter useful for characterization of these systems near a phase transition point. A microscopic scenario of the constituent interactions in terms of the momentum fractions was presented.

The universality of description of the spectra of different hadrons over a wide kinematical region by the scaling function $\psi(z)$ reflects general features (symmetries) of the underlying physical phenomena over a wide scale range. Both soft and hard regimes manifest self-similarity of particle production at a level of hadron constituents. They are preferable to study collective processes and constituent substructure at low and high z, respectively.

The obtained results may be exploited to search for and study of new physical phenomena in particle production in the high energy proton–proton and proton–antiproton collisions at U70, RHIC, Tevatron, and LHC.

Acknowledgments. The investigations have been partially supported by the IRP AVOZ10480505, by the Grant Agency of the Czech Republic under the contract No. 202/07/0079 and by the special program of the Ministry of Science and Education of the Russian Federation, grant RNP.2.1.1.5409.

REFERENCES

1. *Eichten E., Lane K., Peskin M.* // Phys. Rev. Lett. 1983. V. 50. P. 811;
   Eichten E., Hinchliffe I., Lane K., Quigg C. // Rev. Mod. Phys. 1984. V. 56. P. 4.

2. *Meyer A.* The 2007 Europhysics Conference on High Energy Physics // J. Phys. Conf. Ser. 2008. V. 110. P. 072023.

3. *Barrau A., Grain J., Alexeyev S.* // Phys. Lett. B. 2004. V. 584. P. 114.

4. *Mandelbrot B.* The Fractal Geometry of Nature. San Francisco: Freeman, 1982;
   Nottale L. Fractal Space-Time and Microphysics. Singapore: World Sci., 1993;
   Feder J. Fractals. New York: Plenum Press, 1988.

5. *Arsene I. et al.* (*BRAHMS Collab.*) // Nucl. Phys. A. 2005. V. 757. P. 1;
   Back B. B. et al. (*PHOBOS Collab.*) // Nucl. Phys. A. 2005. V. 757. P. 28;

Adams J. et al. (*STAR Collab.*) // Nucl. Phys. A. 2005. V. 757. P. 102;
Adcox K. et al. (*PHENIX Collab.*) // Nucl. Phys. A. 2005. V. 757. P. 184.

6. *Zborovský I., Tokarev M. V.* // Phys. Rev. D. 2007. V. 75. P. 094008.
7. *Stavinsky V. S.* // Sov. J. Part. Nucl. 1979. V. 10. P. 949.
8. *Zborovský I., Tokarev M. V., Panebratsev Yu. A., Škoro G. P.* // Phys. Rev. C. 1999. V. 59. P. 2227.
9. *Antreasyan D. et al.* // Phys. Rev. D. 1979. V. 19. P. 764.
10. *Alper B. et al.* (*BS Collab.*) // Nucl. Phys. B. 1975. V. 100. P. 237.
11. *Büsser F. W. et al.* (*CCRS Collab.*) // Nucl. Phys. B. 1976. V. 106. P. 1.
12. *Drijard D. et al.* (*CDHW Collab.*) // Nucl. Phys. B. 1982. V. 208. P. 1.
13. *Jaffe D. E. et al.* // Phys. Rev. D. 1989. V. 40. P. 2777.
14. *Adams J. et al.* (*STAR Collab.*) // Phys. Rev. Lett. 2003. V. 91. P. 172302.
15. *Adams J. et al.* (*STAR Collab.*) // Phys. Lett. B. 2006. V. 637. P. 161.
16. *Adams J. et al.* (*STAR Collab.*) // Phys. Lett. B. 2005. V. 616. P. 8.
17. *Adams J., Heinz M.* (*for the STAR Collab.*). nucl-ex/0403020.
18. *Tokarev M. V.* // Proc. Intern. Workshop «Relativistic Nuclear Physics: from Hundreds of MeV to TeV», Varna, Bulgaria, September 10–16, 2001. JINR, E1,2-2001-290, Dubna, 2001. V. 1. P. 280–300.
19. *Albrow M. G. et al.* (*CHLM Collab.*) // Nucl. Phys. B. 1973. V. 56. P. 333–345.
20. *Arsene I. et al.* (*BRAHMS Collab.*) // Phys. Rev. Lett. 2004. V. 93. P. 242303.
21. *Tokarev M. V., Zborovský I.* // Yad. Fiz. 2007. V. 70. P. 1335. [Phys. At. Nucl. 2007. V. 70. P. 1294].
22. *Witt R.* (*for the STAR Collab.*) // J. Phys. G: Nucl. Part. Phys. 2005. V. 31. P. S863–S871.
23. *Acosta D. et al.* (*CDF Collab.*) // Phys. Rev. D. 2005. V. 71. P. 032001.
24. *Acosta D. et al.* (*CDF Collab.*) // Phys. Rev. Lett. 2002. V. 88. P. 161802.
25. *Abelev B. I. et al.* (*STAR Collab.*) // Phys. Rev. C. 2007. V. 75. P. 064901.
26. *Guettler K. et al.* (*BSM Collab.*) // Phys. Lett. B. 1976. V. 64. P. 111.
27. *Guettler K. et al.* (*BSM Collab.*) // Nucl. Phys. B. 1976. V. 116. P. 77.

28. *Adams J. et al.* (*STAR Collab.*) // Phys. Rev. Lett. 2004. V. 92. P. 092301.

29. *Adler S. S. et al.* (*PHENIX Collab.*) // Phys. Rev. C. 2007. V. 75. P. 051902(R).

30. *Adams J. et al.* (*STAR Collab.*) // Phys. Lett. B. 2005. V. 612. P. 181.

31. *Adams J. et al.* (*STAR Collab.*) // Phys. Rev. C. 2005. V. 71. P. 064902.

32. *Abelev B. I. et al.* (*STAR Collab.*) // Phys. Rev. C. 2007. V. 75. P. 064901.

33. *Acosta D. et al.* (*CDF Collab.*) // Phys. Rev. Lett. 2003. V. 91. P. 241804.

34. *Tang Z.* (*for the STAR Collab.*). arXiv:0804.4846v1 [nucl-ex];
Adare A. et al. (*PHENIX Collab.*) // Phys. Rev. Lett. 2007. V. 98. P. 3232002.

35. *Zhu L. Y. et al.* (*FNAL E866/NuSea Collab.*). arXiv:0710.2344v1 [hep-ex].

36. *Cleymans J., Redlich K.* // Phys. Rev. C. 1999. V. 60. P. 054908.

37. *Rafelski J.* arXiv:0710.1931v2 [nucl-th] 29 March 2008.

38. *Stanley H. E.* Introduction to Phase Transitions and Critical Phenomena. Oxford: Clarendon Press, 1971.

39. *Patashinsky A. Z., Pokrovsky V. L.* Fluctuation Theory of Phase Transitions. M.: Nauka, 1975.

40. *Ma S.* Modern Theory of Critical Phenomena. W. A. Benjamin, Inc., 1976.

Received on September 23, 2008.

Корректор *Т. Е. Попеко*

Подписано в печать 1.12.2008.
Формат 60 × 90/16. Бумага офсетная. Печать офсетная.
Усл. печ. л. 1,93. Уч.-изд. л. 2,72. Тираж 415 экз. Заказ № 56422.

Издательский отдел Объединенного института ядерных исследований
141980, г. Дубна, Московская обл., ул. Жолио-Кюри, 6.
E-mail: publish@jinr.ru
www.jinr.ru/publish/